

# Pattern dynamics of Rayleigh-Bénard convective rolls and weakly segregated diblock copolymers

Jacob J. Christensen<sup>1</sup> and Alan J. Bray<sup>2</sup>

<sup>1</sup>*Institute of Physics and Astronomy, University of Aarhus, DK-8000 Aarhus C, Denmark*

<sup>2</sup>*Department of Physics and Astronomy, The University of Manchester, Manchester M13 9PL, United Kingdom*

(Received 3 April 1998)

We consider the pattern dynamics of the lamellar phases observed in Rayleigh-Bénard convection, as described by the Swift-Hohenberg equation, and in the weak segregation regime of diblock copolymers. Both numerical and analytical investigations show that the dynamical growth of the characteristic length scale in both systems is described by the same growth exponents, thus suggesting that both systems are members of the same universality class. [S1063-651X(98)03310-8]

PACS number(s): 47.54.+r, 47.27.Te, 64.75.+g, 83.10.Nn

## I. INTRODUCTION

The study of the dynamics of pattern formation in systems far from equilibrium encompasses examples from physics, chemistry, and biology [1]. Despite completely different physical origins, some systems exhibit identical morphologies and pattern dynamics and may be perceived as members of the same universality class.

In this paper we consider the pattern dynamics of two morphologically identical systems, namely, Rayleigh-Bénard convective rolls and weakly segregated diblock copolymers. At short times after a quench from the uniform stable phase to the unstable phase both systems develop a labyrinthine domain morphology consisting of rolls (or lamellae) of a well-defined width  $w$ . Initially the rolls are randomly oriented, but as time increases they locally align in parallel, thereby creating an increasingly ordered pattern (Fig. 1). We have investigated the dynamics of this coarsening process by numerical integration of the appropriate Langevin equations and by analytical considerations. Both approaches agree that the characteristic length scale of the systems scales dynamically with growth exponents that are common to both systems, thereby suggesting that the pattern dynamics of Rayleigh-Bénard convection and diblock copolymers belong to the same universality class.

The observed ordering phenomenon is driven by two mechanisms, namely, interface relaxation and defect annihilation. The effect of the former mechanism can in a defect-free system be calculated by considering the speed at which a modulated interface relaxes to its (straight) ground state. Specifically we apply the projection operator method [2] developed for interface relaxation in the Rayleigh-Bénard system to the same problem in diblock copolymers, thus providing a systematic treatment of both systems. Furthermore, we show how the application of a general approach to interface relaxation recently developed by one of the authors [3] leads to the same result for the Rayleigh-Bénard system.

This paper is organized as follows. In Sec. II we introduce the two models we study. Our numerical work is presented and discussed in Sec. III. Section IV contains the theoretical considerations including a brief review of the projection operator method. Section V concludes with a summary and discussion.

## II. MODELS

In the Rayleigh-Bénard system a simple fluid is confined between two horizontal plates that are heated from below and for values of the Rayleigh number  $R$  larger than a critical value  $R_c$  an instability occurs that transforms the uniform state to a state consisting of spatially periodic convective rolls. Near the onset of the convective instability the free energy functional  $F$  of the Rayleigh-Bénard system is, in dimensionless variables, well approximated by the form

$$F[\phi] = \int d^2r \{ -\phi[\epsilon - (k_0^2 + \nabla^2)^2]\phi/2 + \phi^4/4 \}, \quad (1)$$

deduced by Swift and Hohenberg [4]. Here the scalar order-parameter field  $\phi = \phi(x, y, t)$  is related to the local vertical fluid velocity,  $\epsilon = (R - R_c)/R_c$  is the reduced Rayleigh number that acts as the control parameter of the system, and  $k_0$  is the wave number corresponding to the period  $\lambda = 2w$  of the modulated structure, i.e.,  $k_0 = \pi/w$ .

For small  $\epsilon$  the order parameter field is locally well described by a single-mode approximation  $\phi(\mathbf{r}) \sim \cos(\mathbf{k} \cdot \mathbf{r})$ , where  $\mathbf{k}$  is perpendicular to the orientation of the rolls, and as  $\epsilon \rightarrow 0$  this approximation is exact [5]. Minimizing the free energy Eq. (1) in the single-mode approximation yields  $k = k_0$  as the selected wave number of the steady state. As is customary we use  $k_0 = 1$ . The equation of motion for  $\phi$  is given by the Langevin equation  $\partial_t \phi = -\delta F[\phi]/\delta \phi + \zeta$ , where  $F$  is the above free energy and  $\zeta = \zeta(\mathbf{r}, t)$  is thermal noise correlated as  $\langle \zeta(\mathbf{r}, t) \zeta(\mathbf{r}', t') \rangle = 2A \delta(\mathbf{r} - \mathbf{r}') \delta(t - t')$ , where  $A$  parametrizes the strength of the thermal fluctuations. Thus the Swift-Hohenberg equation reads

$$\partial_t \phi = \epsilon \phi - (k_0^2 + \nabla^2)^2 \phi - \phi^3 + \zeta. \quad (2)$$

A diblock copolymer (DC) is a linear chain molecule joined together by two strings of equal length of, e.g.,  $A$  and  $B$  monomers. The polymerization index  $N$  is thus  $N = N_A + N_B$ , where  $N_A = N_B$  are the numbers of  $A$  and  $B$  monomers, respectively. Above the critical temperature  $T_c$ ,  $A$  and  $B$  mix, whereas below  $T_c$  the two sequences are incompatible and the copolymer melt undergoes phase separation. However, spinodal decomposition [6] cannot continue indefinitely because of the chemical bond between the sequences. As a result, the phase separation occurs on a length

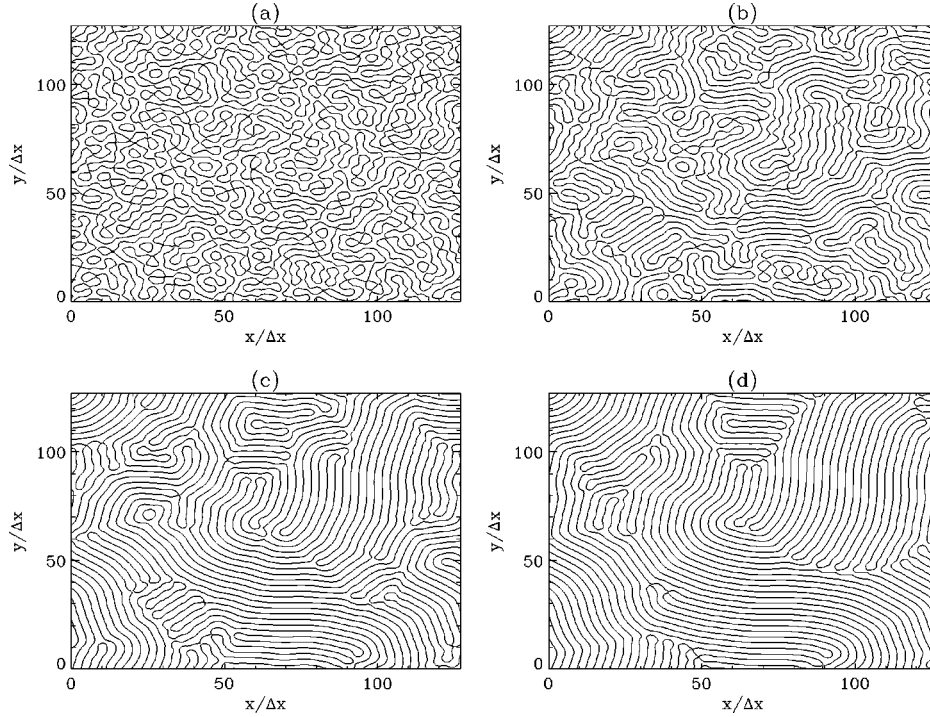


FIG. 1. Coarsening process. The figure shows snapshots of the domain configurations in the diblock polymer system shortly after the quench from the disordered to (a) the bistable phase and at (b)–(d) increasingly later times. The pictures are contour plots of  $128 \times 128$  systems where the contours are defined by  $\phi(x, y, t) = 0$ . The order-parameter field  $\phi(x, y, t)$  was obtained by numerical integration of Eq. (5) at zero thermal noise. Simulations of the Swift-Hohenberg system [Eq. (2)] produces domain configurations that morphologically are indistinguishable from those presented here for the diblock copolymer system.

scale bounded above by the length of a stretched polymer chain (typically less than  $1 \mu\text{m}$ ) where banded domains of  $A$ -rich and  $B$ -rich regions alternate in the final equilibrium state. The free energy of a diblock copolymer melt below  $T_c$  is given (also in dimensionless variables) by a modified Cahn-Hilliard free energy functional [7]

$$F[\phi] = \int d^d r [f(\phi) + (1/2)(\nabla\phi)^2] + (\Gamma/2) \int d^d r d^d r' \phi(\mathbf{r}) G(\mathbf{r}, \mathbf{r}') \phi(\mathbf{r}'), \quad (3)$$

where  $\phi(\mathbf{r}, t) = \phi_A(\mathbf{r}, t) - \phi_B(\mathbf{r}, t)$  is the local concentration difference between the  $A$  and  $B$  monomers,  $f(\phi) = -\phi^2/2 + \phi^4/4$  is the bulk free energy density, and  $\Gamma$  is a control parameter inversely proportional to the square of the polymerization index  $\Gamma \sim 1/N^2$ . Finally, the Green's function  $G(\mathbf{r}, \mathbf{r}')$  in the second integral is defined by the Poisson equation  $\nabla^2 G(\mathbf{r}, \mathbf{r}') = -\delta(\mathbf{r} - \mathbf{r}')$ . The order parameter for this system is a conserved quantity, thus the appropriate Langevin equation for the time evolution of  $\phi$  subsequent to a quench from the disordered to the bistable phase is  $\partial_t \phi = \nabla^2 \delta F[\phi] / \delta \phi + \zeta$  or, inserting Eq. (3),

$$\partial_t \phi = \nabla^2 (-\phi + \phi^3 - \nabla^2 \phi) - \Gamma \phi + \zeta, \quad (4)$$

where the noise  $\zeta$ , representing the effect of thermal fluctuations, has the correlations  $\langle \zeta(\mathbf{r}, t) \zeta(\mathbf{r}', t') \rangle = -2A \nabla^2 \delta(\mathbf{r} - \mathbf{r}') \delta(t - t')$ . For  $\Gamma$  just below the critical value  $\Gamma_c = 1/4$ , Eq. (4) describes the dynamics of weakly segregated lamellar domains with a well-defined width  $w = \pi/k_0$ , where  $k_0$

$= \Gamma^{1/4}$  is the wave number that minimizes the free energy [Eq. (3)] in a single-mode approximation [8].

The diblock copolymer equation [Eq. (4)] can conveniently be rewritten in a form resembling the Swift-Hohenberg equation [Eq. (2)],

$$\partial_t \phi = \epsilon \phi - (1/2 + \nabla^2)^2 \phi + \nabla^2 \phi^3 + \zeta, \quad (5)$$

where  $\epsilon = \Gamma_c - \Gamma$ . Linearizing in Fourier space about  $\phi = 0$  we find, in both Eqs. (2) and (5), that fluctuations  $\delta\phi_k$  in the order parameter decay exponentially  $\delta\phi_k(t) = \delta\phi_k(0) \exp[-\omega_k t]$  with rate  $\omega_k = (\alpha - k^2)^2 - \epsilon$ , where  $\alpha = 1$ , and  $1/2$  for the Swift-Hohenberg (SH) and DC systems, respectively. Thus both systems have a band of wave vectors  $k_- < k < k_+$ ,  $k_{\pm} = \sqrt{\alpha \pm \sqrt{\epsilon}}$ , for which the uniform state is unstable. In the nomenclature of Cross and Hohenberg [1] this means that both systems are stationary periodic, or type  $I_s$ .

### III. SIMULATIONS

We have solved the SH and DC equations numerically using a finite difference scheme on two-dimensional lattices of size  $512 \times 512$ , with periodic boundary conditions. Numerical algorithms for the spatiotemporal evolution of both systems were obtained by replacing, in Eqs. (2) and (5),  $\partial_t \phi(\mathbf{r}, t)$  by  $(\phi_{ij}^{n+1} - \phi_{ij}^n) / \Delta t$  and  $\nabla^2 \phi(\mathbf{r}, t)$  by the discretized Laplacian

$$\nabla^2 \phi_{ij} = \frac{1}{(\Delta x)^2} \left[ \frac{2}{3} \sum_{\text{NN}} + \frac{1}{6} \sum_{\text{NNN}} - \frac{10}{3} \right] \phi_{ij}, \quad (6)$$

which includes contributions from both nearest neighbors and next-nearest neighbors. Here the indices  $i, j$  represent the coordinates  $(x, y)$  and the index  $n$  represents time. A connection to absolute time and spatial coordinates is established through the relationships  $t = n\Delta t$  and  $\mathbf{r} = (i\hat{x} + j\hat{y})\Delta x$ . The specific choice of coefficients in Eq. (6) ensures that the Laplacian, in Fourier space, is isotropic to second order in  $k^2$ , i.e., the form of the Fourier transform  $\Gamma_{\mathbf{k}}$  of Eq. (6) is  $\Gamma_{\mathbf{k}} = -k^2 + \text{const} \times (\Delta x)^2 k^4 + O((\Delta x k^2)^3)$ . For the diblock copolymer system the fluctuation-dissipation relation for the discrete equation can be maintained by generating two independent Gaussian variables  $v_{ij}^{(1)}(n), v_{ij}^{(2)}(n)$  with zero mean and correlations  $\langle v_{ij}^{(a)}(m) v_{kl}^{(b)}(n) \rangle = 2A\Delta t \delta_{i,k} \delta_{j,l} \delta_{m,n} \delta_{a,b}$  and then setting [9]  $\zeta_{ij}(n) = (1/\Delta x)[v_{i+1,j}^{(1)} - v_{i,j}^{(1)} + v_{i,j+1}^{(2)} - v_{i,j}^{(2)}]$ . In the simpler case of the SH equation,  $\zeta_{ij}(n)$  is a Gaussian distributed field with zero mean and correlations  $\langle \zeta_{ij}(m) \zeta_{kl}(n) \rangle = 2A\Delta t \delta_{i,k} \delta_{j,l} \delta_{m,n}$ .

An inherent complication in this type of numerical simulation is the conflicting constraints that the choice of the step sizes is subject to. The need for numerical accuracy requires  $(\Delta x, \Delta t)$  to be vanishingly small, whereas the finite computational power available requires the opposite. Specifically, a linear stability analysis [10] of the above algorithm with the Laplacian given by Eq. (6) shows that, in order to avoid spurious solutions arising from the subharmonic bifurcation, the dimensionless mesh size  $\Delta x$  and time step  $\Delta t$  must satisfy the relation  $\Delta t < 2/[\alpha - 16/3(\Delta x)^2 - \epsilon]$ , where, as before,  $\alpha = 1$  and  $1/2$  for the SH and DC systems, respectively. In practice, the size of  $\Delta x$  is dictated by the smallest length scale in the problem, which is the selected wavelength  $\lambda = 2w$ . In order to avoid lattice pinning it is desirable to have many lattice points per wavelength. This quantity is given by  $\lambda/\Delta x$ , so by lowering  $\Delta x$  any number can be obtained. However, from the above stability relation we see that decreasing  $\Delta x$  below unity drastically reduces the maximum allowable size of the time step and hence increases the required computer time.

We have performed our simulations using the values  $(\epsilon, \Delta x, \Delta t) = (0.25, 2\pi/8, 0.025)$  for the Swift-Hohenberg system and  $(\epsilon, \Delta x, \Delta t) = (0.05, 1.0, 0.05)$  for the diblock copolymer system, where both sets of values satisfy the appropriate stability relations. In the SH system the selected wavelength is approximately  $2\pi$ , so  $\Delta x = 2\pi/8$  gives eight lattice points per wavelength. The corresponding quantity in the DC system, which we consider in the weak segregation limit or small  $\epsilon$ , is approximately 9, since here the selected wavelength is  $\lambda = 2\pi/(1/4 - \epsilon)^{1/4}$ .

Appropriate to a critical quench the systems were initially prepared in the homogeneous single phase state by assigning to each lattice site a small random number uniformly distributed about  $\phi = 0$ . Nonzero temperatures were simulated using the fluctuation strengths  $A = 0.4$  and  $A = 0.1$  for the SH and DC systems, respectively.

#### Dynamical scaling

We monitor the coarsening phenomenon by means of the usual structure factor  $S(\mathbf{k}, t) = |\phi_{\mathbf{k}}(t)|^2$ , where  $\phi_{\mathbf{k}}(t)$  is the Fourier transform of the order parameter. The circularly averaged structure factor  $S(k, t)$  is sharply peaked around the wave vector  $k_0$ , which corresponds to the width of the rolls,

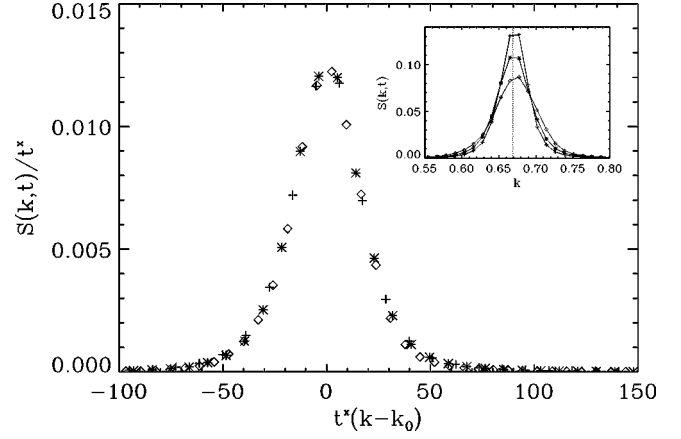


FIG. 2. Test of the scaling form (7) and (inserted) time evolution of the structure factor illustrated with data from simulations of the diblock copolymer system at zero thermal noise (here depicted in arbitrary units). The scaling collapse was obtained with the value  $x = 1/5$  of the scaling exponent. The data sets  $\{\diamond, *, +\}$  represent the (dimensionless) times  $\{1.8 \times 10^4, 5.6 \times 10^4, 1.8 \times 10^5\}$ .

and as time evolves it becomes increasingly sharper and higher. Assuming dynamical scaling, the simplest scaling form for the structure factor is

$$S(k, t) = t^x f(t^x[k - k_0]), \quad (7)$$

where  $f(y)$  is a scaling function. This form implies that the width  $\Delta k$  of the structure factor and its intensity  $S(k_0, t)$  scale as  $\Delta k \sim t^{-x}$  and  $S(k_0, t) \sim t^x$ . In agreement with previous work by a number of authors, our data from the SH system satisfy this scaling form with the scaling exponents  $x = 1/5$  and  $x = 1/4$  at zero and nonzero thermal noise, respectively [2, 11, 12]. Furthermore, we find that the diblock copolymer system also obeys Eq. (7) with the same values of the scaling exponents (Fig. 2).

A more direct method of probing the rolls increasingly orientational order is computing a correlation function  $C_{nn}(\mathbf{r}, t)$ , of the ‘‘nematic’’ order parameter  $\mathbf{n} = \nabla \phi / |\nabla \phi|$ , i.e., the unit vector normal to surfaces of constant  $\phi$  (Fig. 3). Explicitly we have computed the correlation function

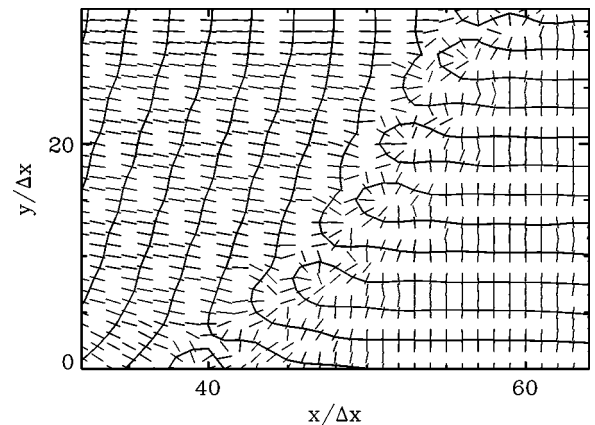


FIG. 3. Local director field  $\mathbf{n}(\mathbf{r}) = \nabla \phi(\mathbf{r}) / |\nabla \phi(\mathbf{r})|$ , here illustrated as small bars, from which the correlation function (8) is computed. For visual clarity only directors near the domain boundaries (solid contours) are depicted.

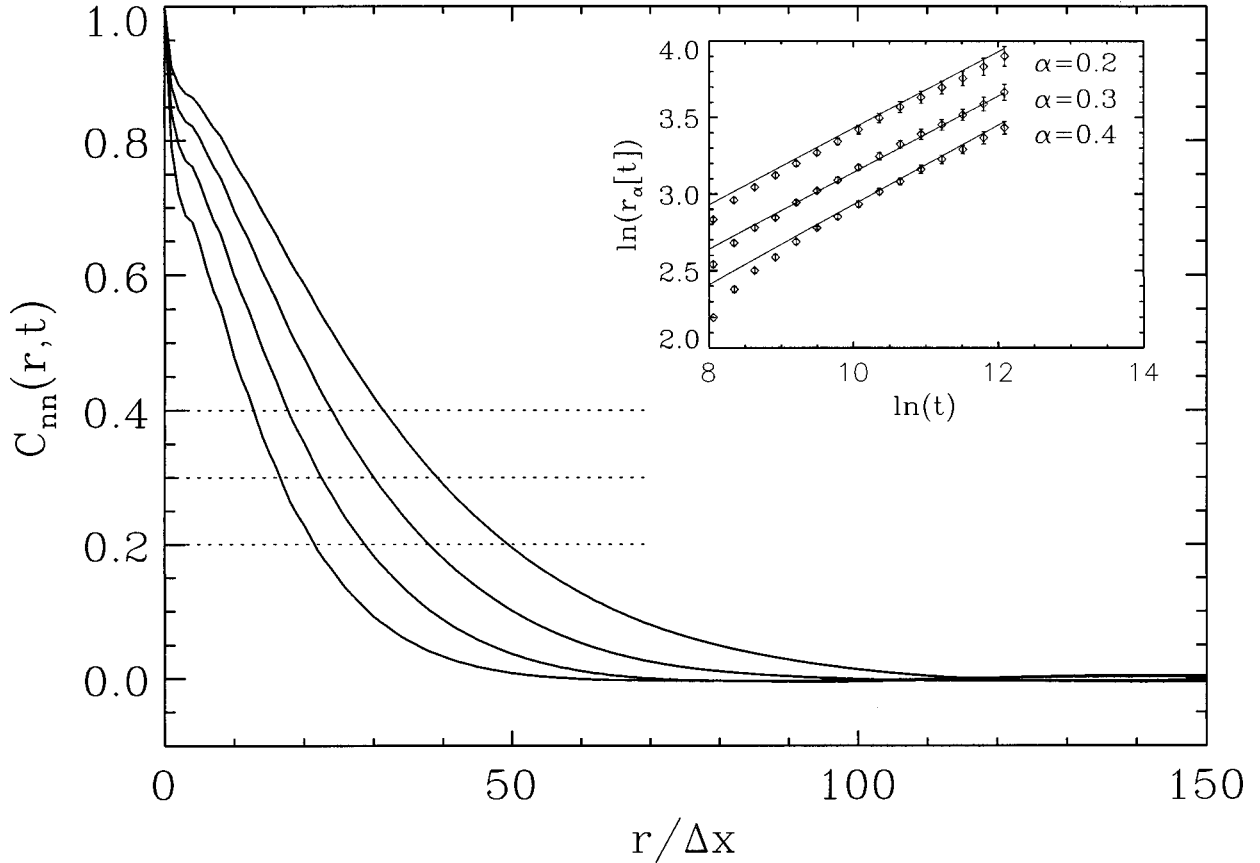


FIG. 4. Time evolution of the director correlation function (8) illustrated with four successive (dimensionless) times  $\{5.6 \times 10^3, 1.8 \times 10^4, 5.6 \times 10^4, 1.8 \times 10^5\}$  increasing from left to right. We extract the time evolution of the length scale  $L(t)$  by monitoring the  $r_\alpha(t)$  for which  $C_{nn}(r_\alpha(t)) = \alpha$ , where  $\alpha < 1$  is some constant (the horizontal dotted lines show  $\alpha = \{0.2, 0.3, 0.4\}$ ). The scaling exponent  $y$  is extracted from a log-log plot of  $r_\alpha(t)$  versus  $t$  (inserted). The data shown result from a simulation of the SH system at zero thermal noise and  $y$  assumes the value  $y = 0.25 \pm 0.02$ .

$$C_{nn}(\mathbf{r}, t) = \frac{2}{N^2} \sum_{\mathbf{x}} \langle [\mathbf{n}(\mathbf{x} + \mathbf{r}, t) \cdot \mathbf{n}(\mathbf{x}, t)]^2 \rangle - 1, \quad (8)$$

where  $N^2$  is the volume of the system and angular brackets denote a statistical average implemented through several independent runs. We compute  $\langle [\mathbf{n}(\mathbf{r}_1) \cdot \mathbf{n}(\mathbf{r}_2)]^2 \rangle$  rather than  $\langle \mathbf{n}(\mathbf{r}_1) \cdot \mathbf{n}(\mathbf{r}_2) \rangle$  since we are interested only in the relative angle  $\theta(\mathbf{r}_1, \mathbf{r}_2)$  between the directors at sites  $\mathbf{r}_1$  and  $\mathbf{r}_2$ . For sites separated by large distances the corresponding directors can be expected to be completely decorrelated and thus  $2\langle \cos^2 \theta \rangle_\theta - 1 = 0$ .

The time complexity of the algorithm for both  $C_{nn}$  and its corresponding structure factor  $S_{nn}(\mathbf{k}, t) = N^{-2} \sum_{\mathbf{r}} C_{nn}(\mathbf{r}, t) \exp(i\mathbf{k} \cdot \mathbf{r})$  is  $N^4$  and with  $N = 512$  excessive computer time is demanded. This problem can be circumvented by introducing the two-dimensional tensor  $Q_{ab}(\mathbf{r}, t) = n_a(\mathbf{r}, t)n_b(\mathbf{r}, t)$ , where  $n_a$ ,  $a = \{x, y\}$  are the components of  $\mathbf{n}$ . In terms of  $Q_{ab}$  Eq. (8) appears as

$$C_{nn}(\mathbf{r}, t) = \frac{2}{N^2} \sum_{\mathbf{x}} \langle Q_{ab}(\mathbf{x} + \mathbf{r}, t) Q_{ab}(\mathbf{x}, t) \rangle - 1, \quad (9)$$

where summation over repeated indices is understood. Since  $S_{nn}$  now has the form  $S_{nn}(\mathbf{k}, t) = 2\langle Q_{ab}(\mathbf{k}, t) Q_{ab}(-\mathbf{k}, t) \rangle - \delta_{\mathbf{k}, 0}$  and  $C_{nn}$  can quickly be computed via  $S_{nn}$  using a fast Fourier transform [13].

The expected scaling form for the correlation function  $C_{nn}$  is

$$C_{nn}(\mathbf{r}, t) = F(r/L(t)), \quad (10)$$

where  $F$  is a scaling function and  $L$  is a length scaling as  $L(t) \sim t^y$ . For both the Swift-Hohenberg and diblock copolymer system we find this scaling form to be satisfied with the scaling exponents  $y = 0.25$  and  $y = 0.30$  at zero and finite noise, respectively (Fig. 4).

The values of the scaling exponent  $y$  agree with the findings of Hou *et al.* [12]. These authors measure the density  $\rho(t)$  of topological defects in the Swift-Hohenberg system and find the algebraic decay  $\rho(t) \sim t^{-y}$ , where  $y = 0.25$  and  $y = 0.30$  at zero and finite noise, respectively. The boundaries between plane-wave domains consist of topological defects. Therefore, the defect density must scale as the perimeter density of the domains, which again scales as the reciprocal  $L^{-1}$  of the linear size of the domains. Furthermore, Hou *et al.* find that the energy of the Swift-Hohenberg system (1) decays as the defect density. Also here the diblock copolymer system behaves as the Swift-Hohenberg system. Measuring the energy, as given by Eq. (3), we find the algebraic decay  $E(t) \sim t^{-y}$  with the same values for  $y$  as above.

#### IV. THEORY

Theoretical analysis of the pattern dynamics of lamellar phases is complicated by the presence of topological defects and current theories apply only to systems without defects. However, locally type  $I_s$  systems exhibit nearly ideal lamellar structures where, in two dimensions, the order parameter can be described as an amplitude modulated plane wave  $\phi(\mathbf{r}, t) = [\phi_0 A(x, y, t) e^{ik_0 x} + \text{c.c.}]$ , where we have assumed lamellae perpendicular to the  $x$  direction;  $A$  is a complex amplitude and c.c. denotes the complex conjugate. Inserting this form into the equations of motion (2) or (5), we obtain in the absence of noise the *amplitude equation*

$$\tau_0 \partial_t A = \epsilon A + \xi_0^2 [\partial_x - (i/2k_0) \partial_y^2]^2 A - g_0 |A|^2 A, \quad (11)$$

where  $\tau_0$ ,  $\xi_0$ , and  $g_0$  are constants. The derivation of Eq. (11) from the Swift-Hohenberg equation (2) is described in Ref. [1] and the method of this reference can easily be extended to the DC equation (5). The amplitude equation describes the dynamics of both the magnitude  $|A|$  and the phase  $\theta(\mathbf{r}, t)$  of the complex amplitude  $A$ . By perturbing the steady state solution of Eq. (11) we obtain, to lowest order in  $\epsilon$ , the *phase equation* [1]

$$\partial_t \theta = D_{\parallel} \partial_x^2 \theta + D_{\perp} \partial_y^2 \theta, \quad (12)$$

where  $D_{\parallel}$  and  $D_{\perp}$  are diffusion coefficients in the parallel and normal directions, respectively. Dimensional analysis of Eq. (12) implies a  $t^{1/2}$  growth of the characteristic length scale, in disagreement with numerical investigations that favor a smaller value of the growth exponent. However, as discussed below, by considering how a curved interface relaxes, working to second order in  $\epsilon$ , a transient regime with  $t^{1/4}$  growth can be predicted.

##### A. Projection operator method

In order to follow the slowly varying orientation of the rolls (or lamellae) Elder *et al.* [2] introduce a coordinate system that tracks the interface given by the points at which  $\phi = 0$ . Specifically, the Cartesian coordinates  $x$  and  $y$  are mapped onto curvilinear coordinates  $(u, s)$ , where  $u$  and  $s$  are locally normal and parallel to the lines  $\phi(\mathbf{r}, t) = 0$ . Assuming that the curvature of the individual rolls is small, the Laplacian in the new coordinates becomes

$$\nabla^2 \simeq \frac{\partial^2}{\partial u^2} + \kappa \frac{\partial}{\partial u} + \frac{\partial^2}{\partial s^2}, \quad (13)$$

where  $\kappa$  is the local curvature. Assuming that the stationary solution of the one-dimensional Swift-Hohenberg equation is a good approximation in the normal direction, Eq. (2) becomes

$$\frac{\partial \phi^s}{\partial u} \frac{\partial u}{\partial t} = 2\kappa \left( \frac{\partial \phi^s}{\partial u} + \frac{\partial^3 \phi^s}{\partial u^3} \right) + \kappa_{ss} \frac{\partial \phi^s}{\partial u} + \Delta, \quad (14)$$

where  $\kappa_{ss} = \partial^2 \kappa / \partial s^2$  and  $\phi^s$  is the solution of  $\phi^s(u(\mathbf{r}, t))^3 = [\epsilon - (k_0^2 + \partial_u^2) \phi^s(u(\mathbf{r}, t))]$ . The final term  $\Delta$  in Eq. (14) contains terms of higher order in  $\kappa$  and terms involving the derivative of  $\kappa$  in the direction normal to the lamellae:  $\Delta$

$= (\kappa_{uu} + \kappa \kappa_u) \partial_u \phi^s + (2\kappa_u + \kappa^2) \partial_u^2 \phi^s$ , where  $\kappa_u$  means  $\partial_u \kappa$ , etc. Application of the projection operator

$$\frac{k_0}{2\pi} \int_{-\pi/k_0}^{\pi/k_0} du \partial_u \phi^s \quad (15)$$

to Eq. (14) produces the final result

$$v = -a\kappa + \kappa_{ss}, \quad (16)$$

where  $v = \partial_t u$  is the interface velocity,  $a = -2(k_0^2 + \beta/\sigma)$ ,  $\sigma = (k_0/2\pi) \int_{-\pi/k_0}^{\pi/k_0} du (\partial_u \phi^s)^2$ , and  $\beta = (k_0/2\pi) \int_{-\pi/k_0}^{\pi/k_0} du (\partial_u \phi^s) (\partial_u^3 \phi^s)$ . The term involving  $\Delta$  drops out from the final result because  $\Delta \partial_u \phi^s$  can be written as  $\partial_u [( \kappa_u + \kappa^2/2) (\partial_u \phi^s)^2]$ , which vanishes when integrated over one lamellar thickness.

In order to evaluate the coefficient  $a$  in Eq. (16) the stationary solution is expanded to leading order in  $\epsilon$ , yielding [5]

$$\phi^s(u) = \Phi_1 \cos(k_0 u) + \Phi_3 \cos(3k_0 u), \quad (17)$$

with coefficients  $\Phi_1 = \sqrt{4\epsilon/3}$  and  $\Phi_3 = -\Phi_1^3/256$ . Using this expansion we find  $a = \epsilon^2/256$ , remembering that  $k_0^2 = 1$ .

Applying the same analysis as above to the DC equation, the equation corresponding to Eq. (14) becomes

$$\frac{\partial \phi^s}{\partial u} \frac{\partial u}{\partial t} = \kappa \left( \frac{\partial \phi^s}{\partial u} + 2 \frac{\partial^3 \phi^s}{\partial u^3} - 3(\phi^s)^2 \frac{\partial \phi^s}{\partial u} \right) + \kappa_{ss} \frac{\partial \phi^s}{\partial u} + \Delta, \quad (18)$$

where  $\phi^s$  is the solution of  $\partial_u^2 \phi^s(u(\mathbf{r}, t))^3 = [\epsilon - (1/2 + \partial_u^2) \phi^s(u(\mathbf{r}, t))]$  and  $\Delta$  has the same meaning as in Eq. (14). Using the projection operator [Eq. (15)], we retrieve Eq. (16), only now with  $a = -(1 + 2\beta/\sigma - 3\gamma/\sigma)$  where  $\gamma = (k_0/2\pi) \int_{-\pi/k_0}^{\pi/k_0} du (\phi^s)^2 (\partial_u \phi^s)^2$  and  $\sigma$  and  $\beta$  are as defined above. The quantities  $\sigma$ ,  $\beta$ , and  $\gamma$  can be determined by substituting the form (17) into the free-energy functional (3) and minimizing with respect to  $k_0$ ,  $\Phi_1$ , and  $\Phi_3$ . To the required order in  $\epsilon = 1/4 - \Gamma$ , the result is  $k_0 = \Gamma^{1/4} = (1/4 - \epsilon)^{1/4}$ ,  $\Phi_1^2 = (8/3)\epsilon + (19/6)\epsilon^2$ , and  $\Phi_3 = -(9/128)\Phi_1^3$ , leading (after some algebra) to  $a = (45/32)\epsilon^2$ , correct to leading nontrivial order in  $\epsilon$ .

In this approximation  $a$  is a very small number,  $a \simeq 2.4 \times 10^{-4}$  and  $a \simeq 3.5 \times 10^{-3}$  in the SH and DC systems when  $\epsilon = 0.25$  and  $\epsilon = 0.05$ , respectively. Dimensional analysis of Eq. (16) therefore implies a crossover in the growth of the characteristic length scale from a transient  $t^{1/4}$  growth to an asymptotic  $t^{1/2}$  growth. The crossover occurs approximately when  $(at)^{1/2} = t^{1/4}$ , that is, when  $t \simeq 1.7 \times 10^7$  in the SH system and when  $t \simeq 8 \times 10^4$  in the DC system. These crossover times far exceed the latest times we have been able to probe in our simulations, but though (as pointed out by Elder *et al.* [2]) an appealing interpretation of the numerical results is that they witness the transient regime, there is no numerical evidence of any crossover behavior. However, since the estimated crossover time for the DC system is three orders of magnitude smaller than the corresponding time in the SH system, the DC system is the obvious candidate for future investigations.

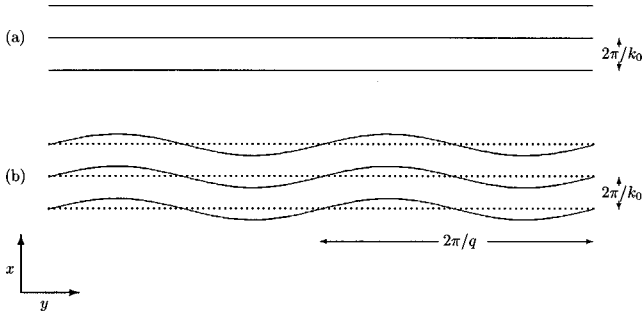


FIG. 5. Sketch of (a) the unperturbed lamellar phase and (b) a modulated lamellar phase. The perturbation  $\tilde{\phi} = A(t)\cos(qy)\psi_q$  introduces spatial variations in the pattern at the length scale  $L = 2\pi/q$ .

### B. Relaxation of a modulated interface

The same problem can be investigated using a general approach to growth exponents recently developed by one of the authors [3]. We consider a small regular perturbation of the perfect lamellar phase and wish to determine the rate at which the system relaxes to its ground state. Setting  $\phi(x, y, t) = \phi_L(x) + \tilde{\phi}(x, y, t)$ , where  $\phi_L(x)$  is the stationary lamellar solution of the Swift-Hohenberg equation (2),

$$0 = \epsilon \phi_L - (k_0^2 + \partial_x^2)^2 \phi_L - \phi_L^3, \quad (19)$$

and  $\tilde{\phi}$  is a small perturbation, the linearized equation of motion for  $\tilde{\phi}$  becomes

$$\partial_t \tilde{\phi} = \epsilon \tilde{\phi} - (k_0^2 + \nabla^2)^2 \tilde{\phi} - 3\phi_L^2 \tilde{\phi}. \quad (20)$$

A modulation of the lamellar phase with wave vector  $q \ll k_0$  is  $\phi(x, y, t) = \phi_L[x + A(t)\cos(qy)] = \phi_L(x) + \phi_L'(x)A(t)\cos(qy)$ , where  $\phi_L'$  means  $\partial_x \phi_L$  and the amplitude  $A$  of the modulation is assumed to be small compared to the lamellar spacing (Fig. 5). More generally, we can write the modulated phase as

$$\phi(x, y, t) = \phi_L(x) + A_0 e^{-\omega_q t} \cos(qy) \psi_q(x), \quad (21)$$

where the function  $\psi_q(x)$  has the same periodicity as  $\phi_L$  [ $\phi_L \sim \cos(k_0 x), k_0 = 1$ ] and satisfies the condition  $\psi_{q=0}(x) = \phi_L'(x)$  since  $q=0$  represents a uniform translation of the lamellae. We have written the time dependence of the amplitude as  $A(t) = A_0 e^{-\omega_q t}$ , describing the decay of the eigenperturbation of the wave vector  $q$  at a characteristic rate  $\omega_q$ .

Insertion of Eq. (21) into Eq. (20) yields an eigenvalue equation  $\hat{H} \psi_q = \omega_q \psi_q$  for the relaxation rate with the Hamiltonian

$$\hat{H} = (k_0^2 + \partial_x^2)^2 + 3\phi_L^2(x) - \epsilon - 2q^2(\partial_x^2 + k_0^2) + q^4. \quad (22)$$

The  $q=0$  mode corresponds to a uniform displacement of the interface wherefore  $\omega_{q=0}$  is fixed to zero. Since  $\psi_0 = \phi_L'$ , this condition corresponds to

$$0 = \epsilon \phi_L' - 3\phi_L^2 \phi_L' - \phi_L' - 2\phi_L''' - \phi_L''''', \quad (23)$$

which is satisfied because Eq. (23) is the derivative of Eq. (19).

In the limit  $\epsilon \rightarrow 0$  we have  $\phi_L \rightarrow 0$ , so for  $\epsilon = 0$  the eigenvalue equation reads  $-\omega_q \psi_q = -(k_0^2 - q^2)^2 \psi_q - 2(k_0^2 - q^2) \psi_q'' - \psi_q''''$ . Remembering that  $\psi_q$  is periodic in  $x$  with wave vector  $k_0$ , this implies  $\omega_q = q^4$ . For small  $\epsilon$  we expect  $\omega_q = a q^2 + q^4$ , where  $a$  is a constant. We can verify this assertion and determine the value of  $a$  by treating the  $q$ -dependent part of  $\hat{H}$  as a perturbation and calculate the first-order correction to the ground state eigenvalue using standard perturbation techniques. The unperturbed eigenfunction for  $\hat{H}$  is  $\psi_0 = \phi_L'$  with eigenvalue zero. Obviously the  $q^4$  term in the perturbation just gives a contribution  $q^4$  to the eigenvalue. The  $O(q^2)$  contribution is

$$\begin{aligned} a q^2 &= -2q^2 \frac{\int dx \phi_L' (\partial_x^2 + k_0^2) \phi_L'}{\int dx (\phi_L')^2} \\ &= 2q^2 \left[ \frac{\int dx (\phi_L'')^2}{\int dx (\phi_L')^2} - k_0^2 \right] \end{aligned}$$

and with  $\phi_L$  expanded as previously [Eq. (17)] we have  $a = \epsilon^2/256$ . Thus the relaxation rate is

$$\omega_q = \frac{\epsilon^2}{256} q^2 + q^4. \quad (24)$$

We notice that the coefficient  $a$  here assumes the same value as determined above by the projection operator method and that a dimensional analysis of Eq. (24) thus predicts the same crossover behavior as did the analysis of Eq. (16) for the interface velocity. Furthermore, we notice that the formal expression for the coefficient  $a$  is identical to that obtained from the projection operator method, as may be seen from an integration by parts, i.e., the result holds generally, not just to the order given by the expansion (17).

Due to the more complicated structure of the DC equation (5), a similar analysis of interfacial relaxation in diblock copolymers has not yet proved possible. The main difficulty is that the Hamiltonian operator  $\hat{H}$  for this case is not self-adjoint, even for  $q=0$ , with the result that a perturbative calculation of  $\omega_q$  requires not only the null eigenfunction  $\phi_L'(x)$  of the  $q=0$  operator  $\hat{H}_0$ , but also the null eigenfunction of the adjoint operator  $\hat{H}_0^\dagger$ , which we have so far been unable to determine.

## V. SUMMARY AND DISCUSSION

By numerical investigations we have found evidence of identical coarsening dynamics for the lamellar phase of the Swift-Hohenberg and diblock copolymer systems. This suggests that both systems belong to the same universality class. We have extracted temperature-dependent dynamical scaling exponents for the characteristic length scale partly by computing the ordinary structure factor and partly by computing a correlation function [Eq. (8)] of the director field. Surprisingly, the two methods yield different scaling exponents indicating that the scaling phenomenon in question is non-

trivial. We have no good understanding of the reasons for this discrepancy, but it should be noticed that the length scale extracted from the structure factor does not have the same immediate geometrical interpretation as has the length scale extracted from the director-field correlation function. Furthermore, the fact that the length scale  $L_{nn}$  arising from the director field correlation function scales with the same growth exponents as the energy suggests that  $L_{nn}$  is the physically important length scale in the system.

Theoretically, by considering how curved interfaces relax we have demonstrated that the projection operator method, when applied to either of the two systems, results in the same scaling exponents. This finding supports the suggestion from our numerical work that the coarsening dynamics of the

Swift-Hohenberg and diblock copolymer systems belong to the same universality class. However, the theoretical analysis applies only to defect-free systems and does not explain the observed temperature dependence of the growth exponents. A thorough understanding of the coarsening phenomenon considered here requires a theoretical treatment that successfully includes the simultaneous effects of both interfacial relaxation and defect-defect interactions.

#### ACKNOWLEDGMENTS

J.J.C. wishes to thank the Theory Group of the Schuster Laboratory, The University of Manchester, for hospitality during a nine month visit.

- 
- [1] M. C. Cross and P. C. Hohenberg, *Rev. Mod. Phys.* **65**, 851 (1994).
  - [2] K. R. Elder, J. Viñals, and M. Grant, *Phys. Rev. Lett.* **68**, 3024 (1992); *Phys. Rev. A* **46**, 7618 (1992).
  - [3] A. J. Bray, *Phys. Rev. E* **58**, 1508 (1998).
  - [4] J. Swift and P. C. Hohenberg, *Phys. Rev. A* **15**, 319 (1977).
  - [5] Y. Pomeau and P. Manneville, *J. Phys. (Paris)* **40**, L609 (1979).
  - [6] A. J. Bray, *Adv. Phys.* **43**, 357 (1994).
  - [7] F. Liu and N. Goldenfeld, *Phys. Rev. A* **39**, 4805 (1989).
  - [8] J. J. Christensen, K. Elder, and H. C. Fogedby, *Phys. Rev. E* **54**, R2212 (1996).
  - [9] R. Petschek and H. Metiu, *J. Chem. Phys.* **79**, 3443 (1983).
  - [10] T. M. Rogers, K. Elder, and R. C. Desai, *Phys. Rev. B* **37**, 9638 (1988).
  - [11] M. C. Cross and D. I. Meiron, *Phys. Rev. Lett.* **75**, 2152 (1995).
  - [12] Q. Hou, S. Sasa, and N. Goldenfeld, *Physica A* **239**, 219 (1997).
  - [13] W. H. Press, S. A. Teukolsky, W. T. Vetterling, and B. P. Flannery, *Numerical Recipes in C, The Art of Scientific Computing*, 2nd ed. (Cambridge University Press, Cambridge, 1992).